Preprint Title	Menthyl esterification allows chiral resolution for synthesis of artificial glutamate analogs
Authors	Kenji Morokuma, Shuntaro Tsukamoto, Kei Miyako, Ryuichi Sakai, Raku Irie and Masato Oikawa
Publication Date	07 Apr 2020
Article Type	Full Research Paper
Supporting Information File 1	SI-2_NMR_sum.pdf; 3.3 MB
Supporting Information File 2	SI-3_X-ray_sum.pdf; 280.5 KB
Supporting Information File 3	X-AA70052-002_XY20170821001.cif; 104.2 KB
Supporting Information File 4	si-1_expmtl.pdf; 606.1 KB
ORCID® iDs	Masato Oikawa - https://orcid.org/0000-0002-3919-811X

Menthyl esterification allows chiral resolution for synthesis of artificial glutamate analogs

Kenji Morokuma[‡1], Shuntaro Tsukamoto[‡1], Kei Miyako[2], Ryuichi Sakai[2], Raku Irie[1], Masato Oikawa[*1]

Address: [1]Yokohama City University, Seto 22–2, Kanazawa–ku, Yokohama 236–0027, Japan and [2]Faculty of Fisheries Sciences, Hokkaido University, Hakodate 041–8611, Japan

Email: Masato Oikawa* - moikawa@yokohama-cu.ac.jp

* Corresponding author

‡ Equal contributors

Abstract

Herein we report enantiospecific synthesis of two artificial glutamate analogs designed based on IKM–159, an antagonist selective to AMPA-type ionotropic glutamate receptor. The synthesis features chiral resolution of the carboxylic acid intermediate by esterification with L–menthol, followed by configurational analysis by NMR, conformational calculation, and X–ray crystallography. Mice in vivo assay showed that (2R)–MC–27 with six-membered oxacycle is neuroactive, whereas the (2S)–counterpart is inactive. It was also found that the TKM–38 with eight-membered azacycle is neuronally inactive to suggest the possibility that the analog with a smaller five-membered azacycle may act as a potent agent.

Keywords

Introduction

Ionotropic glutamate receptor (iGluR) mediates majority of the excitatory neurotransmission in the mammalian central nervous system (CNS), and plays an important role in higher brain functions such as learning and memory [1]. Previously, we have synthetically developed (2*R*)–IKM–159 (**1**) as an artificial glutamate analog that is antagonistic selectively to AMPA-type iGluR (Figure 1) [2,3]. From a series of these studies (see **1**, **2**, and **5** in Figure 1) [3,4], we found that 1) the (2*R*)–enantiomer is responsible for the neuroactivity, and 2) the activity is controlled by the structure of the C–ring; the seven-membered azacyclic analog **2** ((2*R*)–TKM–107) is moderately hypoactive, that is, attenuates voluntary movement of mice upon intracerebroventricular injection, and the seven-membered oxacycle **5** ((2*R*)–IKM– 154) is weakly hypoactive [4].

		size of the C ring		
		6	7	8
heteroatom of the C ring	nitrogen	(2*R*)–**IKM–159** (**1**) AMPA receptor inhibitor [a] *significantly hypoactive in vivo*	(2*R*)–**TKM–107** (**2**) *moderately hypoactive in vivo* [b]	(2*R*)–**TKM–38** (**3**) *inactive in vivo* **this work** [c]
	oxygen	(2*R*)–**MC–27** (**4**) *weakly hypoactive in vivo* **this work**	(2*R*)–**IKM–154** (**5**) *weakly hypoactive in vivo* [b]	*not yet synthesized*
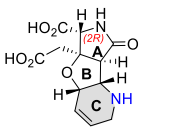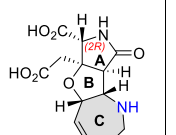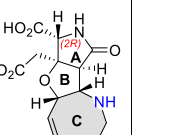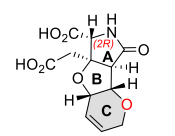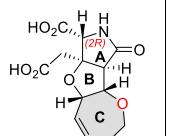
Figure 1: Our artificial glutamate analogs synthesized in an enantiomerically pure form. (a) See references 2 and 3; (b) See reference 4; (c) New analog.

In 2015, we reported synthesis and evaluation of six-membered oxacyclic analog *rac*–**4** (MC–27) in the racemic form, which was shown to be weakly hypoactive in vivo [5]. In the present study, we synthesized both enantiomers of MC–27 (**4/4***, see Figure 1 for the (2*R*)–enantiomer) separately, and found that, as expected, the (2*R*)–enantiomer **4** is responsible for the neuroactivity (see above). Herein, we also report enantiospecific synthesis and evaluation of novel eight-membered azacyclic analog (2*R*)–TKM–38 (**3**, see Figure 1) and the antipode **3***.

For synthesis of enantiomerically pure artificial glutamate analogs, we previously developed enantiospecific synthesis using chiral amine as a starting material, and applied to the synthesis of both enantiomers of IKM–159 (**1** and the antipode) in 2013 [3]. The synthesis reported herein is based on the menthol-mediated chiral resolution which has been de novo developed thereafter for enantiospecific synthesis of seven-membered ring analogs TKM–107 (**2** and the antipode, see Figure 1) and IKM–154 (**5** and the antipode) [4]. Structural analysis of the diastereomeric menthyl esters obtained after chiral resolution had been conducted based on a combination of NOESY data and conformational calculation in that study [4]. In this study, the configurational analysis of the menthyl ester is reasonably justified by X–ray crystallographic analysis, as follows.

Results and Discussion

Enantiospecific synthesis of MC–27

Synthetic route for the racemate of heterotricyclic MC–27 (*rac*–**4**) has been established in 2015 as shown in Scheme 1 [5-7]. Starting from oxanorbornene *rac*–**6** [6,8], the heterotricyclic framework was constructed over five-steps sequence including domino metathesis reaction as a key step to give *rac*–**7**. Subsequent three steps from *rac*–**7** (esterification with CH_2N_2, PMB removal, and ester hydrolysis) had been proven to be promising for preparation of subgram quantities of *rac*–MC–27 (*rac*–**4**), which was found to cause weak inhibition of voluntary movement of mice upon intracerebroventricular injection [5].
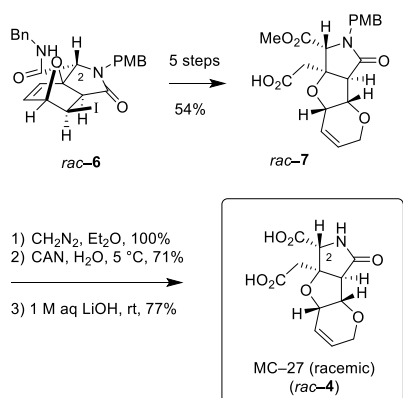
Scheme 1: Our established synthesis route for racemic MC–27 (*rac*–**4**) [5–7].

On the basis of the racemate synthesis shown in Scheme 1, in the present study, we envisioned that the both enantiomers of MC–27 would be independently synthesized from racemic carboxylic acid intermediate *rac*–**7** [6]. For such chiral resolution, we recently discovered that L–(–)–menthol (**8**) is of use as a chiral auxiliary in the enantiospecific synthesis of other analogs **2** and **5** (see Figure 1) [4], and the strategy was found to be also effective here (Scheme 2). Thus, esterification mediated by 2–

methyl–6–nitrobenzoic anhydride (MNBA, Shiina esterification) [9], followed by chromatographic separation of the diastereomers generated, successfully provided **9*** ((2*S*)–isomer, t_R 7.0 min) and **9** ((2*R*)–isomer, t_R 11.5 min) in 45.3% and 44.4% yields, respectively (Figure 2). It should be noted here that DCC and DMAP drove the esterification in poor yield (51% in total for **9** and **9***). As shown in Figure 2, the preparative separation was performed cleanly even in a gram-scale (1.70 g) synthesis. The structures, illustrated in Scheme 2 and Figure 2, were unambiguously determined later from crystallographic and spectroscopic studies of the derivative of **9** (2*R*) (see below).
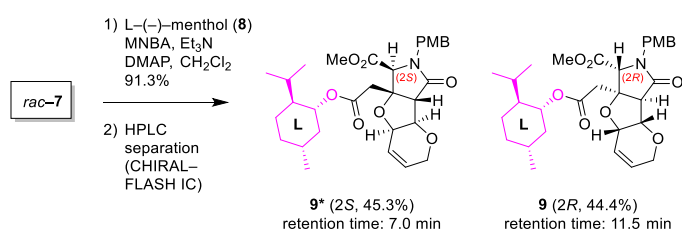
Scheme 2: Resolution of the MC–27 precursor (*rac*–**7**) by chiral auxiliary.
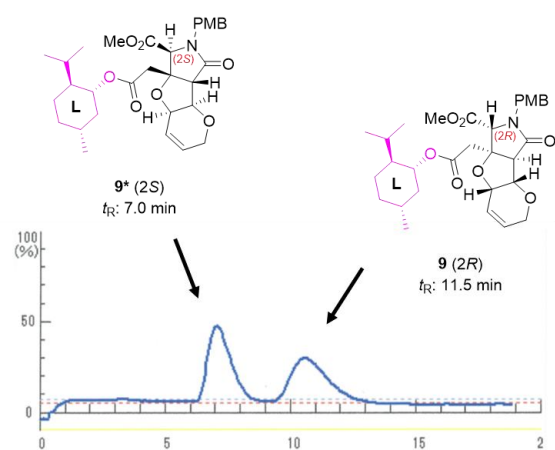
Figure 2: Chiral chromatography profiles for separation of menthyl ester diastereomers **9** and **9***. *Conditions:* 30 × 100 mm CHIRALFLASH IC column, EtOH/hexane = 65/35, 20 mL/min, 25 ˚C, 254 nm, t_R 7.0, 11.5 min.

5

Scheme 3 shows synthesis of (2*R*)–enantiomer of MC–27. Deprotection of the PMB group of **9** (*t*R 11.5 min in Figure 2) by CAN proceeded smoothly at rt to give rise to **10**. The stereochemical configuration of **10** was here determined to be (2*R*), in consideration of the fact that a NOESY cross peak at CO_2Me/Hx observed for **10** was consistent with the top three conformers (total population: 76.5%) for (2*R*)–isomer generated by CONFLEX [10-12] (version 5, MMFF94S, Figure 3). Since **10** was obtained as crystals, the configurational analysis was thereafter confirmed by single-crystal X–ray analysis as shown in Figure 4.
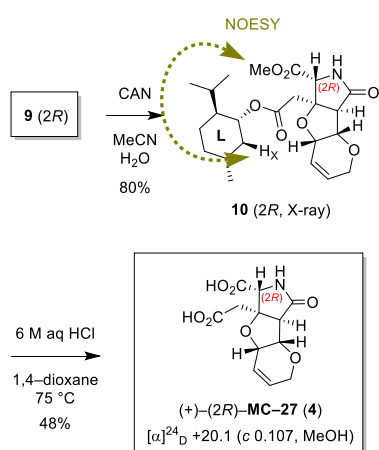
Scheme 3: Final elaboration toward (2*R*)–MC–27 (**4**).
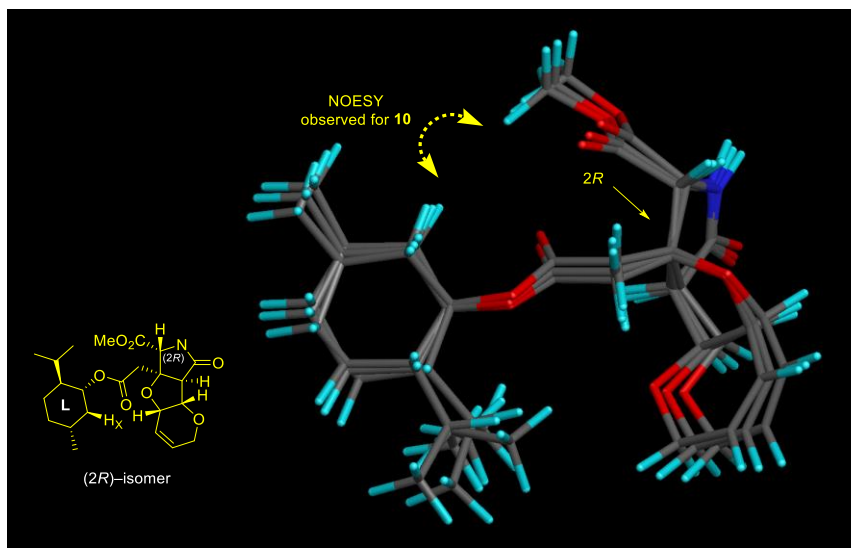
Figure 3: Superimposed structures of the top 3 stable conformers (76.5% total population) generated by CONFLEX (MMFF94S) for (2*R*)–isomer is consistent with the NOESY cross peak observed for **10** (400 MHz, CDCl₃).
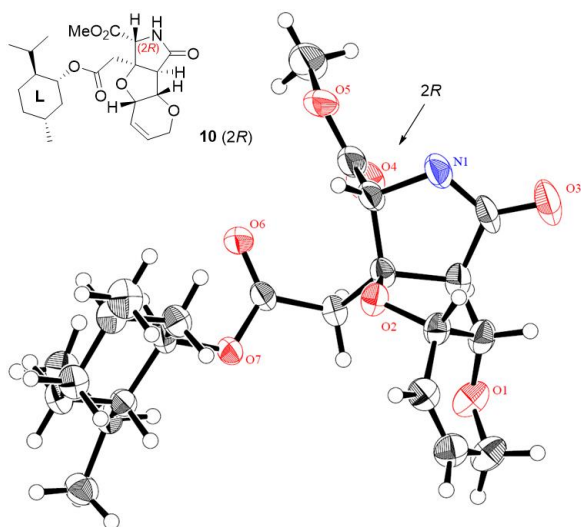
Figure 4: Crystallographic analysis of the menthyl ester **10** unequivocally showed the (2*R*)–configuration (CCDC 1869703).

Hydrolytic deprotections were finally examined to complete the synthesis. Previously employed alkaline hydrolysis (1 M aq LiOH, MeOH or THF, rt→45 °C) [4], however, gave only a monocarboxylic acid product with the menthyl ester remained unaffected

(structure not shown). Fortunately, complete deprotection of two esters was possible cleanly under acidic conditions (6 M aq HCl, 1,4–dioxane, 75 °C, 4 days) to furnish (2*R*)–MC–27 (**4**) in 48% yield (Scheme 3), which was chromatographically and spectroscopically identical to the racemate [5].

On the other hand, *N*–PMB amide **9*** (2*S*) (*t*R 7.0 min in Figure 2) was also deprotected by CAN (Scheme 4), and the configurational analysis of the product **10*** was attempted separately. An important NOESY correlation observed for **10*** is shown also in Scheme 4. The conformational analysis of the (2*S*)–isomer, carried out by CONFLEX (MMFF94S) was, however, not very encouraging, since the four contiguous single bonds between the heterotricycle and the menthyl group were found to be freely rotating in the top five conformers (total population: 94.4%, data not shown). Although a characteristic NOESY cross peak shown in Scheme 4 seemed to be attributed to the second conformer (29.4% population, data not shown) of the (2*S*)–isomer, the other conformers were not consistent well. Due to the conformational flexibility of the (2*S*)–isomer thus presumed, the de novo configurational characterization by spectroscopic analysis in combination with conformational calculation was unsuccessful to conclude that **10*** is the (2*S*)–isomer, separately.
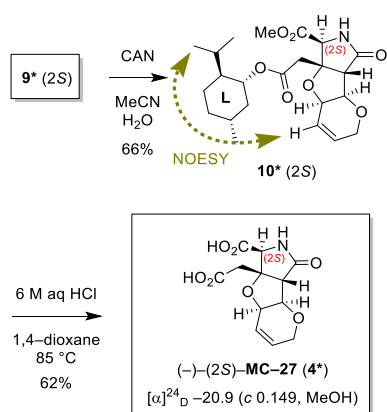
Scheme 4: Synthesis of (2*S*)–MC–27 (**4***) from **9***.

With **10*** (2*S*) in hand, (2*S*)–MC–27 (**4***) was synthesized in reasonable yield (62%) by acidic hydrolysis (Scheme 4). (2*S*)–MC–27 (**4***), thus synthesized, was identical to the antipode **4** (see above) chromatographically and spectroscopically except for the sign of the [α]$_D$ value (see Schemes 3 and 4).

Enantiospecific synthesis of TKM–38

For enantiospecific synthesis of TKM–38 which uniquely bears eight-membered azacycle for the C–ring, we explored 1) the amino-protecting group, and 2) the conditions for cyclization of the medium-sized ring by ring-closing metathesis (RCM). Finally established synthetic route with optimized reaction conditions is shown in Scheme 5. First, direct introduction of pentenyl group to oxanorbornene *rac*–**6** [6,8] proceeds smoothly to give *rac*–**13** in moderate yield (51%), when *N*–(4–pentenyl) TFA amide **12** prepared from 4–pentenyl bromide (**11**) and TFANH$_2$ was reacted in the presence of Cs$_2$CO$_3$ in DMF. We next examined construction of the characteristic eight-membered ring using vinyl acetate and Zhan catalyst–1B (**14**, see Figure 5 for the structure) [13]. Construction of such medium-sized ring is generally highly challenging [14,15], and this was also the case with *rac*–**13**, since we first obtained incomplete triene intermediate *rac*–**15** as a result of only ring-opening metathesis (ROM) mediated by the Fischer-type carbene complex ([Ru]=CH–OAc) [6], generated by the reaction of Zhan catalyst–1B (**14**) with vinyl acetate. Predominant generation of triene *rac*–**15** obviously indicated that the ROM reaction proceeded regioselectively, as also observed in our previous study [6]. With triene *rac*–**15** in hand, cyclization of the eight-membered ring was furthermore attempted by RCM. Gratifyingly, after several trial experiments, we found that the desired cyclization took place smoothly to give rise to heterotricycle *rac*–**16** in 64% yield (for two steps) as a mixture of *E/Z*

isomers (4:1) at the acetoxyalkene moiety, when the reaction conducted with 0.05 equiv of the catalyst **14** at 69 °C. The highly efficient overall conversion of the oxanorbornene *rac*–**13** to the heterotricycle *rac*–**16** through the eight-membered ring formation would be owing to the *cis*-relationships of the pentenyl and vinyl groups on the B–ring of *rac*–**15**, which allows proximal arrangement of the reacting sites in the RCM.
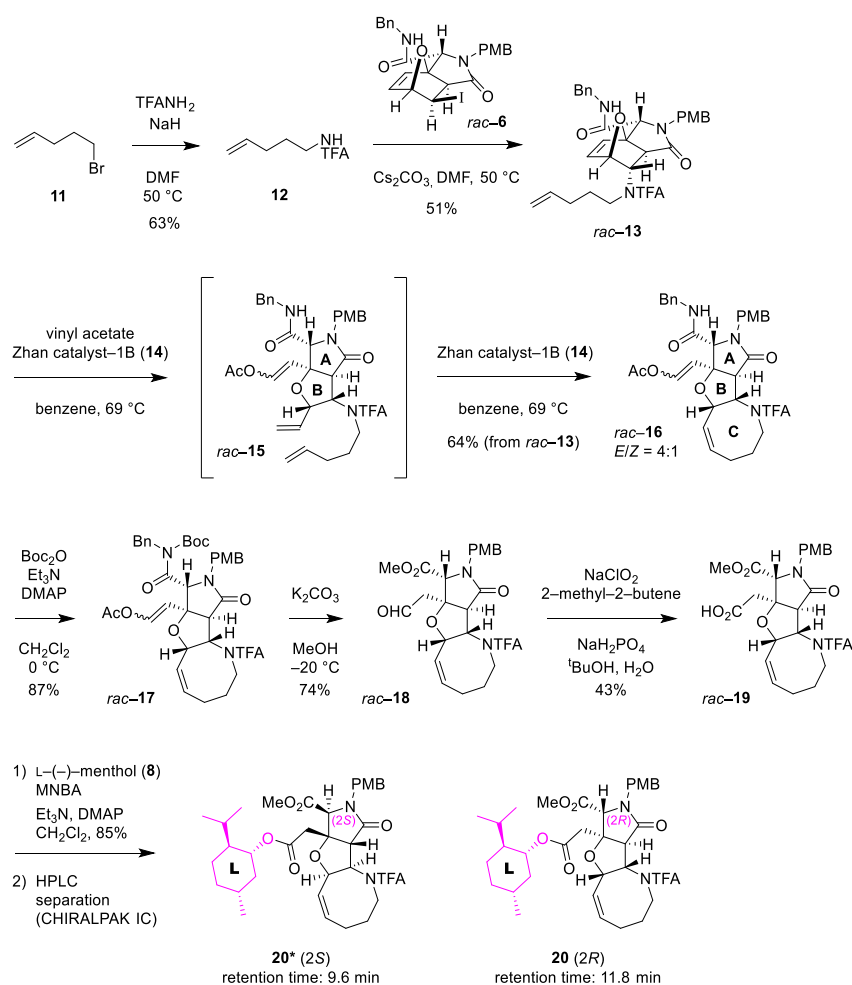
Scheme 5: Construction and chiral resolution of the 5/5/8 ring system toward TKM–38 enantiomers.
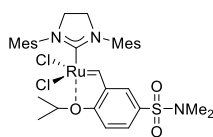
Figure 5: Zhan catalyst–1B (**14**) [13].

N–Boc derivatization of *rac*–**16** (87% yield), followed by alkaline methanolysis (74% yield) [16] and Pinnick oxidation (43% yield) [17-19], delivered carboxylic acid *rac*–**19**. Unfortunately, an attempt to improve the oxidation yield was not fruitful; oxidation of the aldehyde *rac*–**18** with TEMPO [20] resulted in lower yield (28%). The carboxylic acid *rac*–**19** was then esterified with L–(–)–menthol (**8**) for chiral resolution. The reaction was mediated smoothly by MNBA [9] in 85% yield to give a diastereomeric mixture of menthyl esters (**20***, **20**) after silica-gel column chromatography. As shown in Figure 6, clean separation of **20***/**20** was realized by preparative HPLC with CHIRALPAK IC column to furnish **20*** (t_R 9.6 min) and **20** (t_R 11.8 min) in the ratio of 53:46 (**20***/**20**), for which the stereochemical configuration was computationally and spectroscopically determined as (2*S*) and (2*R*), respectively, one step later at **21***/**21** (see below).
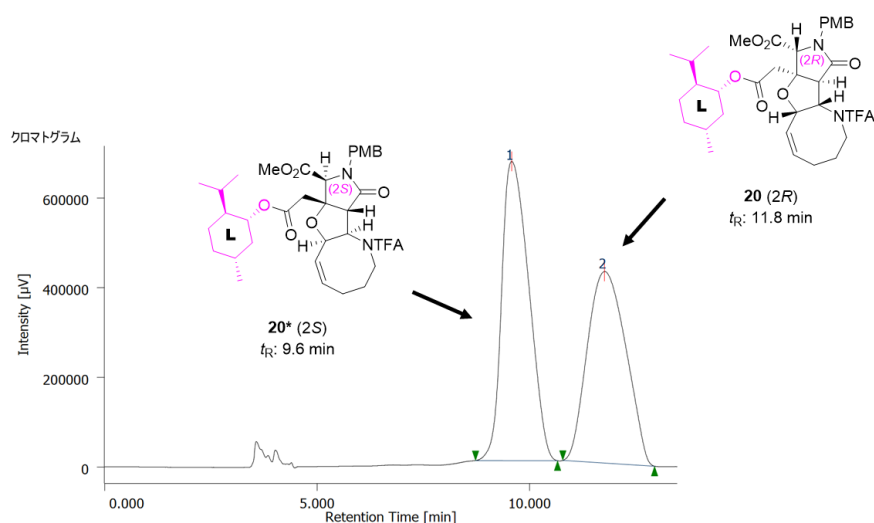
Figure 6: Chiral HPLC profiles for separation of menthyl ester diastereomers **20*** and **20**. *Conditions:* 4.6 × 250 mm CHIRALPAK IC column, EtOH/hexane = 1/19, 1 mL/min, 40 ˚C, 254 nm, t_R 9.6, 11.8 min.

The PMB group of **20*** and **20** was then independently removed by CAN at −10 °C to give **21*** and **21** in 53% and 80% yields, respectively (Scheme 6). With **21*** and **21**, the stereochemistries were determined on the basis of the NOESY data in combination with the conformational analyses by CONFLEX, as follows. Thus, as for **21*** (see Figure 7), three characteristic NOESY cross peaks observed between isopropyl protons and methyl ester protons (Me_A/Me_B, Me_A/Me_C, Me_A/H_D) were found to be reasonably accounted by the top 5 stable conformers (89.9% total population) calculated for (2*S*)–isomer (MMFF). On the other hand, two NOESY cross peaks were observed at Me_A/Me_E and Me_A/H_F for **21** (see Figure 8), which were consistent with the top 5 stable conformers for (2*R*)–isomer (76.8% total population, MMFF). It was thus concluded that **20*** and **21*** are isomers with (2*S*)–configuration, and stereochemistry of **20** and **21** is (2*R*), as described in Figure 6, and Schemes 5 and 6.
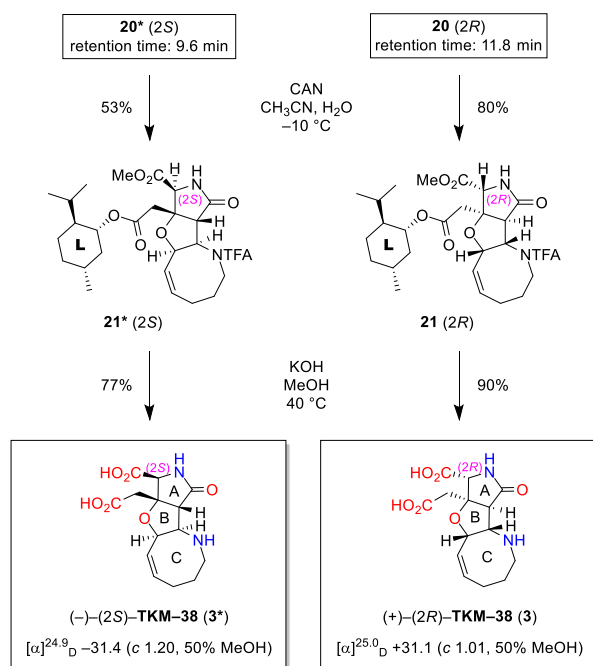
Scheme 6: Final elaboration toward (2*R*)– and (2*S*)–TKM–38.
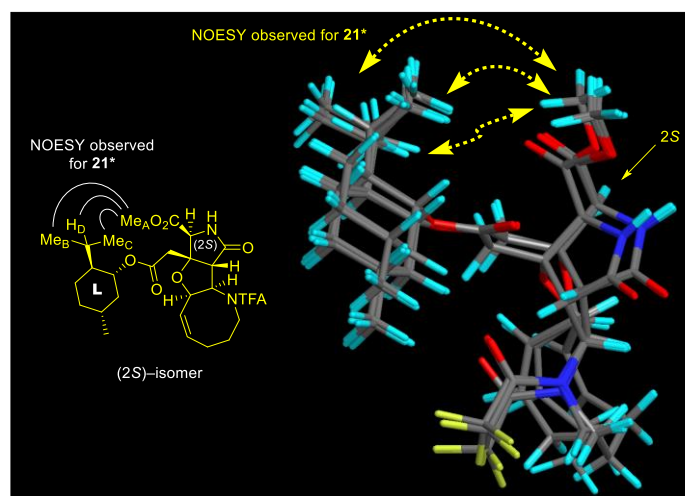
Figure 7: Superimposed structures of the top 5 stable conformers (89.9% total population) generated by CONFLEX (MMFF) for (2*S*)–isomer is consistent with the NOESY cross peaks observed for **21*** (400 MHz, CDCl₃).
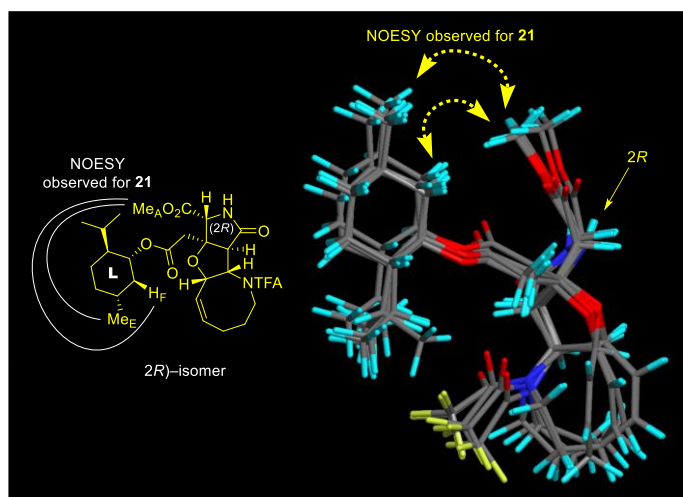
Figure 8: Superimposed structures of the top 5 stable conformers (76.8% total population) generated by CONFLEX (MMFF) for (2R)–isomer is consistent with the NOESY cross peaks observed for **21** (400 MHz, CDCl3).

The stereochemical analyses carried out here and in our previous study [4] have become possible owing to the conformational rigidity of four contiguous single bonds between the heterotricycle and the menthyl ring. The correctness of the analysis has been proven by single-crystal X–ray analysis of MC–27 precursor **10** (2R, Figure 4). Although the isomer **10*** (2S) was analyzed to be rather flexible at the four contiguous single bonds (see above), the larger eight-membered ring here in **21** and **21*** (see Scheme 6) would restrict free rotation at these bonds, thereby both (2R)– and (2S)– isomers were independently identified from NOESY data and CONFLEX calculation. Unfortunately, however, more reliable crystallographic data were available for neither of these intermediates **20*/21*** nor **20/21**, that were obtained as oils.

Finally, hydrolytic removal of menthyl, methyl, and TFA groups were attempted toward both enantiomers of TKM–38 (**3/3***, Scheme 6). Preliminary study with **21*** (2S) showed the low reactivity under acidic conditions (6 M aq HCl, MeOH, 65 °C) [5,21], which

resulted in quantitative recovery of the substrate **21*** (2*S*). We then examined alkaline hydrolysis (KOH, MeOH, H_2O, 40 °C) [22,23], which gratifyingly furnished (2*S*)–TKM–38 (**3***) in good yield (77%) after ion-exchange chromatography (Dowex® 50W x8–200, H^+ form). LiOH, that was used for final deprotection in the synthesis of MC–27 (**4** and **4***, see Schemes 3 and 4), was not capable of facilitating removal of the TFA group of **21*** (2*S*). The procedure with KOH also provided the (2*R*)–enantiomer (**3**) of TKM–38, from **21** (2*R*) in 90% yield.

The neuronal activities

Mice behavioral activity was evaluated with artificial glutamate analogs synthesized in this study. Intracerebroventricular injection (50 µg/mouse) of (2*R*)–MC–27 (**4**) caused weak inhibition of the voluntary action of mouse, which had been observed previously with *rac*–MC–27 with nearly identical potency [5]. It was, therefore, concluded that the (2*R*)–enantiomer is responsible for the neuroactivity of *rac*–MC–27.

On the other hand, neither of the enantiomers of the new analog TKM–38 (**3/3***) bearing eight-membered azacycle showed behavioral activity; no effects were observed on the voluntary action of mice upon intracerebroventricular injection (50 µg/mouse).

Conclusion

We showed here in detail that ester formation of the carboxylic acid intermediates *rac*–**7** and *rac*–**19** with L–(–)–menthol (**8**) [4] enables chiral resolution of our heterotricyclic artificial glutamate analogs more practically than our previous method using chiral amine as a starting material [3]. The correctness of the configurational analysis on **10** (2*R*) based on NOESY data and conformational calculation was undoubtedly proven by the crystallographic data (see Figure 4) in the present study, justifying the propriety of the analyses in a series of the studies [4] employing menthol-mediated chiral resolution as well.

The mice in vivo assay in the present study has shown that, as for MC–27 (**4**), the (2*R*)–isomer is the neuroactive enantiomer. It is again interesting that (2*R*)–isomer is neuronally active, because (2*S*)–isomer is generally neuroactive for glutamic acid and some natural products with glutamate motif, dysiherbaine [24] and kainic acid [25]. Since (2*R*)–isomer is the neuronally active enantiomer in these analogs (see Figure 1), our future studies will straightforwardly focus on the enantioselective synthesis of the only (2*R*)–isomer. Asymmetric Ugi reaction recently developed [26] is of interest for selective preparation of (2*R*)–**6** (see Schemes 1 and 5) [6,8]. Studies are in progress to develop asymmetric Ugi/Diels–Alder reaction, and the results will be reported in due course.

The in vivo inactivity of TKM–38 (**3**) found in this study shows the less potent neuroactivity of analogs with larger C–ring (see analogs **1**–**3** in Figure 1). The neuroactivity of the new analog **22** with smaller five-membered azacycle for the C–ring (Figure 9) is, therefore, of interest, and the synthesis is also underway in our laboratory.

16
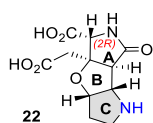
Figure 9: The ongoing synthesis target **22** is expected to show potent neuroactivity.

Experimental

Procedures for all chemical syntheses are described in the Supporting Information File 1.

Mice in vivo behavioral assays

Mice in vivo assay was performed under approval by the Ethical Committee of Experimental Animal Care at Hokkaido University. All experiments were performed in compliance with the relevant laws and institutional guidelines.

An aqueous solution (20 μL) of sample was injected intracerebroventricularly in male ddY mice of 3 to 4 weeks (Japan SLC Inc, Hamamatsu) as described previously [27]. Effects on the behavior of mice were evaluated according to our reported procedures [3].

Supporting Information

Supporting Information File 1:

File Name: si-1_expmtl.docx

File Format: docx

Title: Synthetic procedures

Supporting Information File 2:

File Name: SI-2_NMR_sum.pdf

File Format: pdf

Title: NMR spectra for all new compounds

Supporting Information File 3:

File Name: SI-3_X-ray_sum.pdf

File Format: pdf

Title: X–ray structure for menthyl ester **10**

Supporting Information File 4:

File Name: X-AA70052-002_XY20170821001.cif

File Format: cif

Title: a CIF file for X—ray structure of menthyl ester **10**

Funding

References

1. Riedel, G.; Platt, B.; Micheau, J. *Behav. Brain. Res.* **2003**, *140*, 1-47. doi:10.1016/s0166-4328(02)00272-3

2. Gill, M. B.; Frausto, S.; Ikoma, M.; Sasaki, M.; Oikawa, M.; Sakai, R.; Swanson, G. T. *Br. J. Pharmacol.* **2010**, *160*, 1417-1429. doi:10.1111/j.1476-5381.2010.00784.x

3.   Juknaite, L.; Sugamata, Y.; Tokiwa, K.; Ishikawa, Y.; Takamizawa, S.; Eng, A.; Sakai, R.; Pickering, D. S.; Frydenvang, K.; Swanson, G. T.; Kastrup, J. S.; Oikawa, M. *J. Med. Chem.* **2013**, *56*, 2283-2293. doi:10.1021/jm301590z

4.   Tsukamoto, S.; Itagaki, H.; Morokuma, K.; Miyako, K.; Ishikawa, Y.; Sakai, R.; Oikawa, M. *Heterocycles* **2020**, *101*, 91-98. doi:10.3987/COM-19-S(F)2

5.   Chiba, M.; Fujimoto, C.; Sakai, R.; Oikawa, M. *Bioorg. Med. Chem. Lett.* **2015**, *25*, 1869–1871. doi:10.1016/j.bmcl.2015.03.037

6.   Oikawa, M.; Ikoma, M.; Sasaki, M.; Gill, M. B.; Swanson, G. T.; Shimamoto, K.; Sakai, R. *Eur. J. Org. Chem.* **2009**, *2009*, 5531-5548. doi:10.1002/ejoc.200900580

7.   Oikawa, M.; Ikoma, M.; Sasaki, M.; Gill, M. B.; Swanson, G. T.; Shimamoto, K.; Sakai, R. *Bioorg. Med. Chem.* **2010**, *18*, 3795-3804. doi:10.1016/j.bmc.2010.04.044

8.   Ikoma, M.; Oikawa, M.; Gill, M. B.; Swanson, G. T.; Sakai, R.; Shimamoto, K.; Sasaki, M. *Eur. J. Org. Chem.* **2008**, *2008*, 5215-5220. doi:10.1002/ejoc.200800704

9.   Shiina, I.; Kubota, M.; Oshiumi, H.; Hashizume, M. *J. Org. Chem.* **2004**, *69*, 1822-1830. doi:10.1021/jo030367x

10.   CONFLEX, Version 5; Conflex Corporation: Tokyo-Yokohama, Japan, 2004.

11.   Goto, H.; Ōsawa, E. *J. Am. Chem. Soc.* **1989**, *111*, 8950-8951. doi:10.1021/ja00206a046

12.   Gotō, H.; Ōsawa, E. *J. Chem. Soc., Perkin Trans. 2* **1993**, 187-198. doi:10.1039/P29930000187

13.   Zhan, Z.-Y. Ruthenium complex ligand, ruthenium complex, carried ruthenium complex catalyst and the preparing methods and the use thereof. WO Patent 2007003135, January 11, 2007.

14.   Bracegirdle, S.; Anderson, E. A. *Chem. Soc. Rev.* **2010**, *39*, 4114-4129. doi:10.1039/C0CS00007H

15.   Kleinke, A. S.; Webb, D.; Jamison, T. F. *Tetrahedron* **2012**, *68*, 6999-7018. doi:10.1016/j.tet.2012.05.081

16.   Flynn, D. L.; Zelle, R. E.; Grieco, P. A. *J. Org. Chem.* **1983**, *48*, 2424-2426. doi:10.1021/jo00162a028

17.   Kraus, G. A.; Taschner, M. J. *J. Org. Chem.* **1980**, *45*, 1175-1176. doi:10.1021/jo01294a058

18.   Bal, B. S.; Childers Jr, W. E.; Pinnick, H. W. *Tetrahedron* **1981**, *37*, 2091-2096. doi:10.1016/s0040-4020(01)97963-3

19.   Dalcanale, E.; Montanari, F. *J. Org. Chem.* **1986**, *51*, 567-569. doi:10.1021/jo00354a037

20.   Uesugi, S.-i.; Watanabe, T.; Imaizumi, T.; Ota, Y.; Yoshida, K.; Ebisu, H.; Chinen, T.; Nagumo, Y.; Shibuya, M.; Kanoh, N.; Usui, T.; Iwabuchi, Y. *J. Org. Chem.* **2015**, *80*, 12333-12350. doi:10.1021/acs.joc.5b02256

21.   Chiba, M.; Ishikawa, Y.; Sakai, R.; Oikawa, M. *ACS Comb. Sci.* **2016**, *18*, 399-404. doi:10.1021/acscombsci.6b00046

22.   Badorrey, R.; Cativiela, C.; Diaz-de-Villegas, M. D.; Gálvez, J. *Tetrahedron: Asymmetry* **1995**, *6*, 2787-2796. doi:10.1016/0957-4166(95)00368-Y

23.   Tverezovsky, V. V.; Baird, M. S.; Bolesov, I. G. *Tetrahedron* **1997**, *53*, 14773-14792. doi:10.1016/S0040-4020(97)00988-5

24.   Sakai, R.; Kamiya, H.; Murata, M.; Shimamoto, K. *J. Am. Chem. Soc.* **1997**, *119*, 4112-4116. doi:10.1021/ja963953z

25.   Murakami, S.; Takemoto, T.; Shimizu, Z. *YAKUGAKU ZASSHI* **1953**, *73*, 1026-1028. doi:10.1248/yakushi1947.73.9_1026

26.   Zhang, J.; Yu, P.; Li, S.-Y.; Sun, H.; Xiang, S.-H.; Wang, J.; Houk, K. N.; Tan, B. *Science* **2018**, *361*, eaas8707. doi:10.1126/science.aas8707

27.   Sakai, R.; Swanson, G. T.; Shimamoto, K.; Green, T.; Contractor, A.; Ghetti, A.; Tamura-Horikawa, Y.; Oiwa, C.; Kamiya, H. *J. Pharmacol. Exp. Ther.* **2001**, *296*, 650-658.